



[biblio.ugent.be](http://biblio.ugent.be)

The UGent Institutional Repository is the electronic archiving and dissemination platform for all UGent research publications. Ghent University has implemented a mandate stipulating that all academic publications of UGent researchers should be deposited and archived in this repository. Except for items where current copyright restrictions apply, these papers are available in Open Access.

This item is the archived peer-reviewed author-version of:

Title: Prolonged gene silencing by combining siRNA nanogels and photochemical internalization

Authors: Raemdonck K., Naeye B., Høgset A., Demeester J., De Smedt S.C.

In: Journal of Controlled Release, 145(3), 281-288 (2010)

Optional: link to the article

**To refer to or to cite this work, please use the citation to the published version:**

**Authors (year). Title. *journal Volume(Issue)* page-page. Doi:** 10.1016/j.jconrel.2010.04.012

## **Prolonged gene silencing by combining siRNA nanogels and photochemical internalization**

K. Raemdonck,<sup>a</sup> B. Naeye,<sup>a</sup> A. Høgset,<sup>b</sup> J. Demeester,<sup>a</sup> Stefaan C. De Smedt<sup>a,\*</sup>

<sup>a</sup>Laboratory of General Biochemistry and Physical Pharmacy, Ghent Research Group on Nanomedicines (GRGN), Department of Pharmaceutics, Faculty of Pharmaceutical Sciences, Ghent University, Harelbekestraat 72, B-9000 Ghent, Belgium

<sup>b</sup>PCI Biotech, Hoffsvæien 48, N-0377, Oslo, Norway

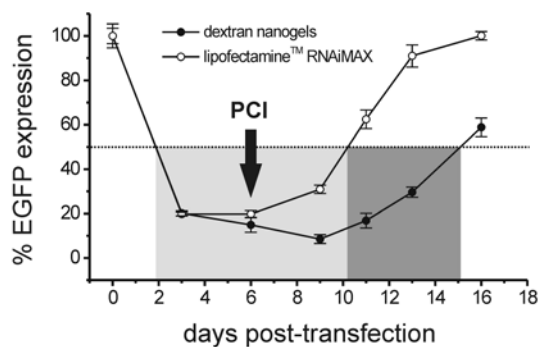
\*Corresponding author: [stefaan.desmedt@ugent.be](mailto:stefaan.desmedt@ugent.be), Laboratory of General Biochemistry and Physical Pharmacy, Ghent Research Group on Nanomedicines (GRGN), Department of Pharmaceutics, Faculty of Pharmaceutical Sciences, Ghent University, Harelbekestraat 72, B-9000 Ghent, Belgium – Phone: +32 (9) 264 80 76 – Fax: +32 (9) 264 81 89.

## Abstract

Small interfering RNAs (siRNAs) show potential for the treatment of a wide variety of pathologies with a known genetic origin through sequence-specific gene silencing. However, siRNAs do not have favorable drug-like properties and need to be packaged into nanoscopic carriers that are designed to guide the siRNA to the cytoplasm of the target cell. In this report biodegradable cationic dextran nanogels are used to deliver siRNA across the intracellular barriers. For the majority of non-viral siRNA carriers studied so far, endosomal confinement is identified as the most prominent hurdle, limiting the full gene silencing potential. Thus, there is a major interest in methods that are able to enhance endosomal escape of siRNA to improve its intracellular bioavailability. Photochemical internalization (PCI) is a method that employs amphiphilic photosensitizers to destabilize endosomal vesicles. We show that applying PCI at a later time-point post-transfection significantly prolonged the knockdown of the target protein only in case the siRNA was carried by nanogels and not when a liposomal carrier was used. Combining siRNA nanogels and PCI creates new possibilities to prolong gene silencing by using intracellular vesicles as depots for siRNA and applying PCI at the time when maintaining the RNAi effect becomes critical.

## Graphical abstract

Combining siRNA nanogels and photochemical internalization (PCI) creates new possibilities to prolong gene silencing by using intracellular vesicles as depots and applying PCI at the time when maintaining the RNAi effect becomes critical.



## Keywords

siRNA, nanogels, transfection, endosomal escape, photochemical internalization, prolonged effect

## Abbreviations

*AEMA*, 2-aminoethyl methacrylate hydrochloride; *AF647*, alexa fluor® 647; *dex-HEMA*, dextran hydroxyethyl methacrylate; *dex-MA*, dextran methacrylate; *DEPC*, diethyl pyrocarbonate; *DLS*, dynamic light scattering; *DS*, degree of substitution; *DsiRNA*, Dicer

substrate siRNA; *EGFP*, enhanced green fluorescent protein; *Huh-7*, human hepatoma-7; *PCI*, photochemical internalization; *PS*, photosensitizer; *RNAi*, RNA interference; *siRNA*, small interfering RNA; *TMAEMA*, [2-(methacryloyloxy)-ethyl]trimethylammonium chloride.

## Introduction

Since the discovery of RNA interference (RNAi) [1], intensive research on RNAi therapeutics and their potential applications has led to an astonishing progress in just over a single decade. This resulted in a fast transition of promising lead siRNA candidates from in vitro tests to clinical trials [2-4]. Advances are made, both in the area of siRNA design [5-9] and siRNA delivery. New formulation strategies emerge, designed to overcome intra- and extracellular hurdles and to improve the fraction of the administered siRNA dose that eventually reaches the cytoplasm of the target cell [3,10-12].

One of the limitations of non-viral carriers for synthetic siRNA delivery, especially when long-term treatment is advised, is the transient nature of the gene silencing effect as a result of cell division and intracellular siRNA degradation [13-16]. On the other hand, major concerns are raised with regard to adverse effects of siRNA therapeutics, such as unwanted immune activation [17], off-target silencing [18] and saturation of the RNAi machinery [19]. As these effects are concentration-dependent it is obvious that delivery of siRNA requires rigorous control over the intracellular siRNA concentrations [13,20]. As a consequence, delivery strategies that are able to control the amount of siRNA that is released in the cytoplasm as a function of time could be of interest to obtain a prolonged gene silencing and/or to minimize side-effects. While the magnitude of target gene (or protein) suppression, relative to a control sample, may be a good indicator for the success of an siRNA treatment, looking at the time-window during which the siRNA therapeutic intervention is able to keep the intracellular protein titers below a certain threshold, is perhaps a better parameter to decide on the efficacy of the delivery strategy [14]. The duration of the silencing effect will eventually strongly determine the dosage frequency in chronic clinical therapy.

During the last decade, an increasing number of publications describes nanoscopic hydrogels as drug delivery carriers, though only a few reports are available on nanogels for siRNA delivery [21]. In this report, cationic dextran nanogels loaded with siRNA are studied [22]. Following in vitro transfection of cells with siRNA loaded cationic nanogels (**Fig. 1**) we observed that a major fraction of the internalized nanogels is trafficked towards acidified vesicles (presumably endolysosomes), which may limit the full potential of RNAi [22]. Here we set out to evaluate if these intracellular vesicles, packed with siRNA nanogels, can be used as a siRNA depot from which siRNA can be released at the desired time in order to prolong the gene silencing effect. In this way the siRNA dose that is taken up by the target cells could be far more efficiently deployed.

As a trigger to induce endosomal escape of siRNA, we applied photochemical internalization (PCI). PCI is a technique that promotes endosomal escape of a variety of therapeutic molecules, such as chemotherapeutics, proteins and nucleic acids and has already proven to enhance gene transfer and RNAi silencing with viral and non-viral nanocarriers. Upon incubation with cells, the photosensitizer (PS) predominantly localizes in the endosomal membrane. Excitation of the PS to its singlet state can be followed by intersystem crossing to its triplet state, of which the energy may be used in photochemical or photophysical reactions. This results in the emergence of reactive oxygen species (ROS),

predominantly singlet oxygen ( $^1\text{O}_2$ ) that may catalyze the oxidation of amino acids, unsaturated fatty acids and cholesterol. Due to its short diffusion range ( $\sim 10\text{-}20$  nm) and its short lifetime ( $0.01\text{-}0.04$   $\mu\text{s}$ ), singlet oxygen initiates oxidation reactions mainly in the local production area [23-26]. This oxidative damage eventually breaks down the endosomal barrier, allowing the transition of internalized nanosized matter into the cytoplasm.

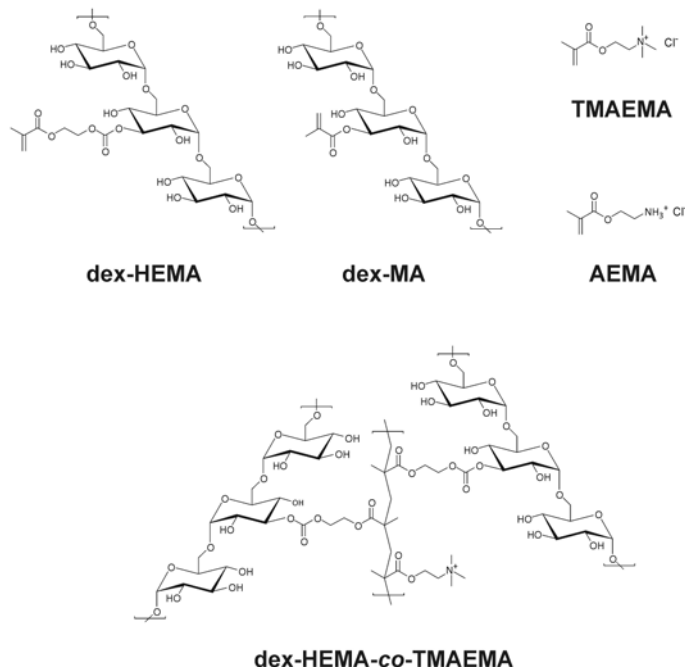


**Fig. 1.** Chemical structures of dextran hydroxyethyl methacrylate (dex-HEMA), [2-(methacryloyloxy)-ethyl]trimethylammonium chloride (TMAEMA), 2-aminoethyl methacrylate hydrochloride (AEMA) and dextran methacrylate (dex-MA). Radical polymerization results in the formation of a hydrogel network, which is shown for dex-HEMA-co-TMAEMA. To prepare cationic nanogels dex-(HE)MA is copolymerized with TMAEMA (and/or AEMA) by a mini-emulsion photopolymerization (see Supplementary Information) [22,27]. While dex-HEMA based nanogels are biodegradable (through hydrolysis of the carbonate ester) dex-MA based nanogels are not as it does not contain a labile ester bond between the methacrylate moiety and the dextran backbone [22,27,28]. Nanogels are loaded with siRNA by rehydrating a weighed amount of nanogel lyophilizate with HEPES buffer and mixing the resulting dispersion with an equal volume of siRNA solution. Dex-HEMA and dex-MA are prepared with varying degree of substitution (DS), being the number of (HE)MA crosslinks per 100 glucopyranose units.

## Materials and methods

### *siRNA duplexes*

Twenty-one nucleotide siRNAs targeting the pGL3 firefly luciferase gene (siLUC), the enhanced green fluorescent protein (siEGFP) and a universal negative control duplex

(siCONTROL) were purchased from Eurogentec (Seraing, Belgium) and stored in 20  $\mu$ M aliquots in DEPC treated water (-20°C). siLUC: sense strand = 5'-CUUACGCUGAGUACUUCGAtt-3'; antisense strand = 5'-UCGAAGUACUCAGCGUAAGtt-3'. siEGFP: sense strand = 5'-CAAGCUGACCCUGAAGUUCtt-3'; antisense strand = 5'-GAACUUCAGGGUCAGCUUGtt-3'. siCONTROL: sense strand = 5'-UGCGCUACGAUCGACGAUGtt-3'; antisense strand = 5'-CAUCGUCGAUCGUAGCGCAtt-3'.

Dicer substrate RNAs (DsiRNAs), chemically modified, targeting the EGFP gene (DsiEGFP) and a universal negative control with the same modification pattern (DsiNC-1) were provided by Integrated DNA technologies (IDT, Leuven, Belgium). DsiEGFP: sense strand = 5'-pACCCUGAAGUUCAUCUGCACCACcg-3'; antisense strand = 5'-pCGGUGGUGCAGAUUGAACUUCAGGGUCA-3'. DsiNC-1: sense strand = 5'-pCGUUAUCGCGUAUAAUACGCGUat-3'; antisense strand = 5'-pAUACGCGUAUUAUACGCGAUUAACGAC-3'. Lower case bold letters represent 2'-deoxyribonucleotides, capital letters are ribonucleotides and underlined capital letters are 2'-O-methylribonucleotides. Lyophilized DsiRNAs were dissolved in HEPES 30 mM pH 7.5 supplemented with 100 mM KAc (100 mM), annealed and stored at -20°C. For fluorescence microscopy experiments, a green fluorescent siRNA duplex was ordered from Dharmacon (siGLO® green transfection indicator).

### ***Preparation of cationic dextran nanogels and loading with siRNA***

Cationic dextran nanogels (dex-HEMA-co-TMAEMA) were prepared using the UV induced emulsion photopolymerization as described in our previous work [22], with minor adjustments. Dex-HEMA (65 mg) was dissolved in a solution containing 40  $\mu$ L irgacure 1% (w/v), 80  $\mu$ L TMAEMA (75% w/v) and 80  $\mu$ L HEPES buffer (pH 7.4, 20 mM). The obtained dex-HEMA solution was emulsified in 5 mL pre-cooled mineral oil, supplemented with 5% (v/v) of ABIL EM 90 as emulsifier. Following sonification (Branson sonifier, 30 s - 20%), the emulsion was exposed to UV light during 15 min under cooling ( $\sim$ 4°C). The prepared nanogels were obtained in pure form by precipitation with acetone:hexane (1:1) and centrifugation. After washing, the precipitate was redispersed in 5 mL distilled water and traces of organic solvent were removed by vacuum evaporation. To assure long-term stability, the nanogels were lyophilized and stored desiccated. Note that for the preparation of the dex-MA nanogels the same protocol was followed using dex-MA instead of dex-HEMA.

The thus obtained nanogels were subsequently loaded with siRNA ('post-loading'). Therefore a stock dispersion of nanogels ( $\sim$ 2 mg/mL) was prepared in ice-cooled HEPES buffer and sonicated to loosen the gel particles (20 s, 10% output power). From this stock dispersion, dilutions were prepared according to the experimental needs. Subsequently, equal volumes of nanogels and siRNA were mixed at room temperature and left to stand at room temperature for  $\geq$  15 min to allow complexation.

Fluorescent labelling of nanogels was performed by copolymerization of dex-MA (DS 5.9) with a 4:1 molar ratio of TMAEMA:AEMA. The nanogels were fluorescently tagged by incubating them with Alexa Fluor® 647 (AF647) succinimidyl ester (Molecular Probes), followed by extensive dialysis against distilled water (Spectra/Por® Float-A-Lyzer® 100.000 MWCO) to remove unreacted dye.

### ***Dynamic light scattering (DLS) and zeta-potential***

Nanogel sizes, polydispersity and surface charge were determined by dynamic light scattering (DLS) and zeta-potential measurements respectively, using a Zetasizer Nano ZS (Malvern, Worcestershire, UK), operating with Dispersion Technology Software (DTS). The samples were equilibrated at 25°C prior to measurement and measurement settings were set on automatic. To screen the degradation of the nanogels, nanogel suspensions (500 µg/mL) were prepared in respectively 20 mM HEPES buffer (pH 7.4) in a low volume cuvette that was subsequently sealed with parafilm. The nanogel suspensions were kept at 37°C and the intensity of the scattered light was measured every 5 minutes. Each measurement time point consisted of 6 runs, with 5 s per run.

### ***Cell lines and culture conditions***

All cellular experiments were performed on Huh-7 hepatoma cells. The wild-type cells are denoted as Huh-7\_wt. Huh-7\_LUC cells stably express the *firefly* and *renilla* luciferase gene [22]. Huh-7\_EGFP cells stably produce the enhanced green fluorescent protein [27]. All cells are grown in DMEM:F12, supplemented with 2 mM glutamine, 10% heat-inactivated fetal bovine serum (FBS, Hyclone) and 100 U/mL penicilline/streptomycine at 37°C in a humidified atmosphere containing 5% CO<sub>2</sub>.

### ***Photochemical internalization***

The photosensitizer (PS) *meso*-tetraphenylporphine disulfonate (TPPS<sub>2a</sub>) was kindly provided by Dr. A. Høgset (PCI Biotech, Oslo, Norway). The PS was protected from light and stored at 4°C until use. Activation of the PS occurred by exposure to blue light (375 nm – 450 nm) emitted by LumiSource® (Osram 18W/67, 13 mW/cm<sup>2</sup>, PCI Biotech, Oslo, Norway).

### ***Luciferase gene silencing***

Two days before transfection, Huh-7\_LUC cells were seeded in 96-well plates (1 x 10<sup>4</sup> cells per well). For transfection, first 90 µL of pre-heated OptiMEM (37°C) was pipetted on the cells and subsequently 10 µL of a siRNA loaded nanogel dispersion (in HEPES buffer) was added to the cells in each well (20 pmol of siRNA). After 4 h incubation (37°C), the nanogels were removed from the cells and replaced with 150 µL pre-heated cell culture medium. This transfection protocol was performed in duplicate (plate 1 and plate 2 respectively) for every sample tested. Twenty-four hours later, the cells on plate 1 were lysed with 20 µL passive lysis buffer (Promega, Leiden, The Netherlands). *Firefly* and *renilla* luciferase activities were determined with the Promega Dual-Luciferase® Reporter Assay. For luciferase analysis we used a GloMax™ 96 luminometer with two injectors. Briefly, 10 µL of cell lysate was mixed with 50 µL *firefly* luciferase substrate and after a 2 s delay, *firefly* luminescence was integrated during 10 s (relative light units or RLU). Subsequently, 50 µL of *renilla* luciferase substrate in Stop & Glo Buffer (Promega) was added and again after 2 s *renilla* luminescence was quantified during a 10 s time interval. For each sample, the ratio of *firefly* luminescence to *renilla* luminescence was calculated. The ratios obtained with siLUC nanogels were compared to the ratios obtained with siCONTROL nanogels and expressed as remaining luciferase expression (%).

The cells on plate 2 were trypsinized with 100  $\mu$ L trypsin/EDTA (0.25%) and replated in 5 separate 96-well plates. Four of these plates are analyzed for luciferase expression on day 2 till day 5 following transfection. On day 5, the trypsinization step was repeated on the remaining 96-well plate in order to avoid overgrowth of the cells and to maintain the cells in a state of active cell division. Luciferase expression was additionally analyzed at day 6 and day 7.

### ***EGFP gene silencing***

#### *EGFP silencing with DS 2.5 nanogels*

Two days before transfection,  $7.5 \times 10^4$  Huh-7\_EGFP cells were seeded in 12-well plates. At the day of transfection, the culture medium was replaced with 900  $\mu$ L pre-heated OptiMEM. DS 2.5 siEGFP nanogel complexes were prepared in HEPES buffer (~20 min incubation at room temperature) and added to the wells to obtain a final volume of 1 mL. The nanogel and siEGFP concentration on the cells eventually equaled 60  $\mu$ g/mL and 75 pmol/mL respectively. As controls, 'empty' nanogels or nanogels loaded with siCONTROL and siLUC were included in the transfection experiment. After 5 h incubation at 37°C, the transfection medium was replaced with 2 mL of complete cell culture medium. Five days post-transfection, the cells were washed with PBS and collected for flow cytometry by trypsinization (500  $\mu$ L trypsin/EDTA 0.25% per well, followed by dilution in 5 mL cell culture medium). After centrifugation (1200 rpm, 7 min) the cell pellet was resuspended in 300  $\mu$ L flow buffer and kept on ice until flow analysis. The cells were analyzed using a Beckman Coulter Cytomics™ FC500 flow cytometer. Dead cells were discriminated from viable cells by the addition of propidium iodide (Invitrogen). The data were analyzed using Beckman Coulter CXP analysis software.

#### *Dose response EGFP silencing with DS 5.2 cationic nanogels*

Huh-7\_EGFP cells were seeded in 24-well plates ( $3 \times 10^4$  cells per well). Two days after seeding, the cells were transfected with 50  $\mu$ g/mL nanogels (500  $\mu$ L in OptiMEM) during 4 h after which the medium was replaced with 500  $\mu$ L of fresh complete cell culture medium. We verified for the DS 5.2 nanogels that 4 h incubation with the cells was the optimal incubation time. Longer incubation did not improve the RNAi activity but rather induced more cytotoxic effects (data not shown). The amount of siEGFP per well was varied between 0.025 pmol and 125 pmol. Nanogels that complex siLUC were used as a control. At day 3 post-transfection, the cells were prepared for flow cytometry by trypsinization (250  $\mu$ L trypsin/EDTA 0.25% per well, followed by dilution in 1 mL cell culture medium). After centrifugation (1200 rpm, 7 min) the cell pellet was resuspended in 200  $\mu$ L flow buffer and kept on ice until flow cytometry analysis as explained above.

#### *EGFP gene silencing kinetics*

Huh-7\_EGFP cells were seeded in 24-well plates at a density of  $5 \times 10^4$  cells per well. Twenty-four hours later, the cells were incubated during 4 h with DS 2.5, DS 5.2 and DS 8.9 nanogels (50  $\mu$ g/mL), loaded with siEGFP or siLUC (50 pmol per well) in a final volume of 500  $\mu$ L (OptiMEM). Lipofectamine™RNAiMAX complexes were prepared in OptiMEM and included in the transfection experiment (1.56  $\mu$ L RNAiMAX stock per well). For all samples, the transfection was performed in duplicate. Subsequently, the transfection medium was



replaced with 500  $\mu$ L cell culture medium. EGFP expression was quantified at different time-points post-transfection. At every time-point, the cells in the duplicate transfection were again replated in two new 24-well plates (1:3 diluted) to be analyzed/replated at the next time-point.

#### *Silencing EGFP studied by fluorescence microscopy*

$1.5 \times 10^4$  Huh-7\_EGFP cells were grown on Lab-Tek™ II chambered cover glasses (Nalge Nunc International, Rochester, NY) two days pre-transfection. As described above, the siRNA:nanogel complexes were prepared in HEPES buffer as a 10x stock dispersion. The transfection was performed by incubating the cells during 4 h with 50  $\mu$ g/mL DS 5.2 nanogels, loaded with 40 pmol siEGFP in a final volume of 400  $\mu$ L OptiMEM and after this incubation period, the remaining complexes were removed and 400  $\mu$ L of fresh cell culture medium was added per well. The same controls as indicated in the above paragraph were used. After 96 h, the cells were washed with PBS and fixed in 4% paraformaldehyde solution (20 min incubation at RT). Subsequently, after three additional washing steps with PBS, the cover glasses were mounted with Vectashield® DAPI mounting medium (Vector Labs). EGFP expression was visualized by fluorescence microscopy using a Nikon EZC1-si confocal scanning module installed on a motorized Nikon TE2000-E inverted microscope (Nikon Benelux, Brussels, Belgium) with open pinhole setting.

#### *Influence of photochemical internalization on EGFP gene silencing kinetics*

The effect of PCI on the silencing duration was evaluated in three distinct protocols where PCI was conducted at the day of transfection (PCI t0), two days or six days post-transfection (PCI t2 and PCI t6 respectively). More details on the protocol time-scale can be found in **supplementary information Fig. S5-6**. For the transfection,  $5 \times 10^4$  cells were seeded in 24-well plates and left to grow for 48 h. Transfection of the cells (in 500  $\mu$ L OptiMEM) was performed with DS 5.2 cationic nanogels at varying concentration. The amount of siRNA (siEGFP and siLUC) per well was 50 pmol. Reminiscent of previous transfections, an incubation period of 4 h with the cells was respected.

#### ***Photochemical internalization studied by fluorescence microscopy***

Huh-7\_wt cells transfected with dex-HEMA-co-TMAEMA (DS 3.2) nanogels were visualized by fluorescence microscopy respectively before and after they were treated with PCI. For this experiment  $12.5 \times 10^4$  Huh-7\_wt cells were seeded in Lab-Tek™ II chambered coverglasses (Nalge Nunc International, Rochester, NY), two days before transfection. One day pre-transfection, PS was added to half of the wells (0.4  $\mu$ g/mL). At the day of transfection, the PS was removed and the cells were washed with PBS. Cationic nanogels were loaded with fluorescent siGLO® in hepes buffer as indicated earlier and incubated with the cells in 400  $\mu$ L OptiMEM. The final concentration of nanogels and siGLO® was 25  $\mu$ g/mL and 200 pmol/mL respectively. After 3 h incubation, the remaining complexes were removed and replaced with complete cell culture medium (37°C). One hour of incubation later, the culture chambers were illuminated with LumiSource® (45s). The cells were placed at 37°C for another 36 h, protected from light. Afterwards, the cell-bound siGLO® fluorescence was quenched by treatment with 0.4% trypan blue (8 min) and after washing with PBS the cells were fixed with 4% paraformaldehyde (20 min, RT). Following 3 washing steps with PBS, the

cells were mounted with Vectashield® DAPI Mounting Medium (Vector Labs, UK) and kept at 4°C (dark) until fluorescence imaging.

### Statistical analysis

All transfection measurements are minimally performed in triplicate and expressed as mean  $\pm$  SD. A paired t-test was conducted to assess the statistical significance in the PCI experiments.

## Results and Discussion

Cationic dextran nanogels with different crosslink density were obtained through the use of dex-(HE)MA with a different DS. The size and zeta-potential of the nanogel batches can be found in **Table 1**. By dynamic light scattering (DLS) we showed that dex-HEMA nanogels dispersed in buffer gradually degrade while dex-MA nanogels do not, as expected (**supplementary information\_Fig. S1**).

A good complexation of the negatively charged siRNA to the cationic dex-HEMA-co-TMAEMA nanogels is a prerequisite to successfully deliver siRNA across the plasma membrane into the cytosol. To evaluate this, the nanogel samples listed in Table 1 were titrated with siRNA and the resultant zeta-potential of the siRNA loaded nanogels was measured. Clearly, the loading of the nanogels with siRNA is reflected in the zeta-potential value as can be seen in the typical sigmoidal curves that are obtained (**Fig. 2**).

**Table 1.** Size and surface charge of the dex-HEMA-co-TMAEMA nanogels. Analysis was performed in HEPES buffer (pH 7.4, 20 mM) with a final nanogel concentration of 0.2 mg/mL. Values are the average  $\pm$  SD of at least 3 measurements on the same sample.

dextran sample	$d_h$ (nm) <sup>a</sup>	PDI	$\zeta$ -potential (mV)
dex-HEMA DS 2.5	254 $\pm$ 5	0.081 $\pm$ 0.055	24.1 $\pm$ 0.7
dex-HEMA DS 3.2	267 $\pm$ 8	0.274 $\pm$ 0.026	27.9 $\pm$ 0.9
dex-HEMA DS 5.2	212 $\pm$ 1	0.106 $\pm$ 0.029	24.8 $\pm$ 0.4
dex-HEMA DS 8.9	207 $\pm$ 1	0.137 $\pm$ 0.034	17.1 $\pm$ 0.7
dex-MA DS 3.4	219 $\pm$ 5	0.105 $\pm$ 0.012	30.2 $\pm$ 0.8
dex-MA DS 5.9 <sup>b</sup>	195 $\pm$ 8	0.196 $\pm$ 0.014	27.2 $\pm$ 0.6

<sup>a</sup>hydrodynamic diameter, <sup>b</sup>dex-MA-co-TMAEMA modified with 20% AEMA for fluorescent labeling with Alexa Fluor® 647, PDI = polydispersity index, DS = degree of (HE)MA substitution

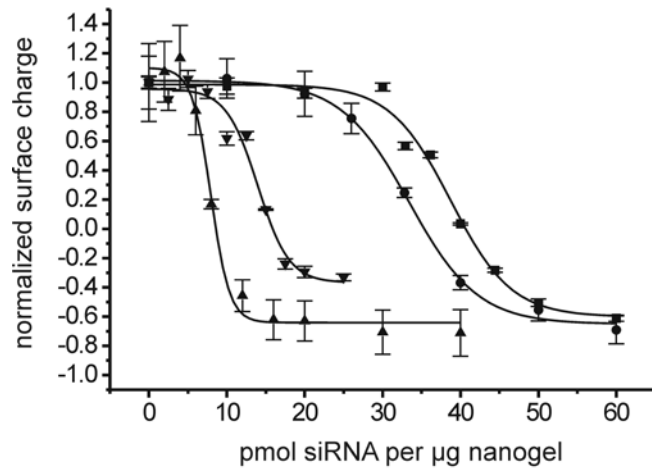


**Fig. 2.** Titration of nanogel dispersions with increasing amounts of siRNA. From left to right: DS 8.9 (▲) – DS 2.5 (▼) – DS 5.2 (●) – DS 3.4 (■). Line graphs represent a Boltzmann sigmoidal fit (Microcal Origin v 5.0). Measurements are performed at 25°C in HEPES buffer 20 mM, pH 7.4. The zeta-potential of the siRNA loaded nanogels was normalized to the zeta-potential of the unloaded nanogels.

Apparently, the nanogels behave differently in their siRNA complexation. Nanogels with DS 5.2 (dex-HEMA) and DS 3.4 (dex-MA) display a decrease in zeta-potential at substantially higher siRNA amounts compared with DS 2.5 and DS 8.9 nanogels. It indicates that the latter nanogels are able to load less siRNA molecules per  $\mu\text{g}$  nanogel lyophilisate. This may be due to e.g. some dex-HEMA hydrolysis during nanogel production (especially in case of the lowly crosslinked DS 2.5 nanogels). Also, the lower zeta-potential in case of the DS 8.9 nanogels (see Table 1) may explain the lower siRNA loading capacity of these nanogels. Alternatively, their high crosslinking degree could potentially exclude the siRNAs from the core of the nanogels leading to a decrease in the maximal siRNA loading capacity.

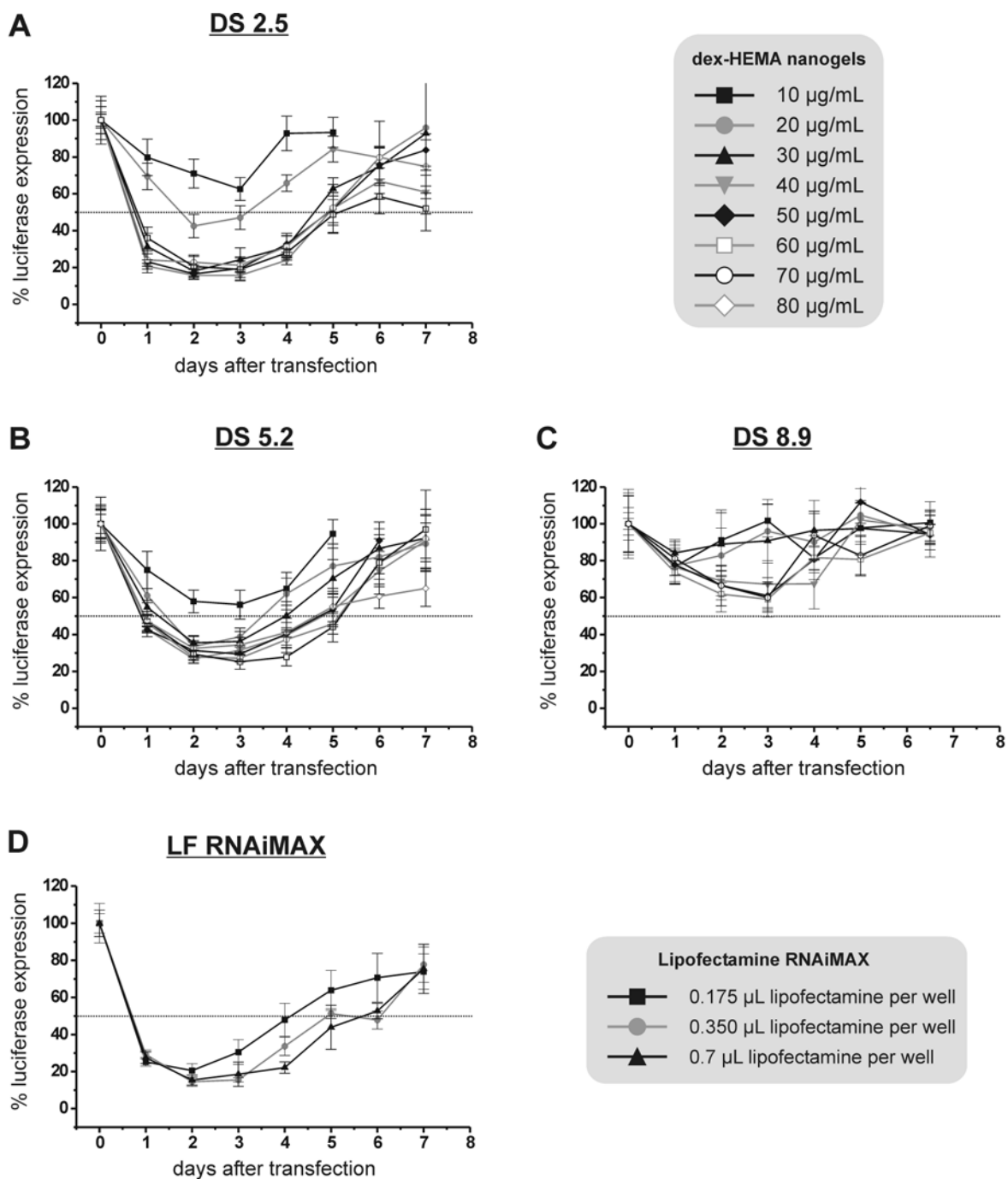


**Fig. 3.** Gene silencing kinetics by siRNA loaded dex-HEMA-co-TMAEMA nanogels, as a function of the DS of the nanogels (**A**: DS 2.5, **B**: DS 5.2, **C**: DS 8.9) and siRNA complexed with Lipofectamine™ RNAiMAX (**D**). ~~To allow a more easy comparison of the luciferase gene silencing kinetics, the data obtained with different nanogel concentrations (30 µg/mL till 70 µg/mL) and lipofectamine™ RNAiMAX (all 3 concentrations tested) were averaged and summarized in (E).~~ Transfection experiments were performed in a 96-well plate format with a fixed amount of siRNA (20 pmol) per well. Data points represent average values ± SD (n=4).

The RNAi activity of the siRNA loaded nanogels (Table 1, **Fig. 3**) was subsequently evaluated in Huh-7 cells, stably expressing both *firefly* and *renilla* luciferase (Huh-7\_LUC cells) [22]. The

sequence of the active siRNA was designed to selectively reduce *firefly* luciferase expression. The siRNA induced knockdown of *firefly* luciferase was normalized to the *renilla* luciferase expression which should not be affected by the active siRNA (see also supplementary information). Luciferase expression was followed during one week after applying siRNA nanogels on the cells (Fig. 3). To maintain the cells in a state of active cell division and prevent cellular overgrowth, we replated the cells at day 1 and day 5 post-transfection. As a positive control, the RNAi gene silencing induced by Lipofectamine™RNAiMAX was evaluated as well.

Fig. 3 (A-C) demonstrates a substantial downregulation of *firefly* luciferase for all nanogels tested. Nanogels with a higher crosslink density (DS 8.9) showed less gene silencing (< 50% knockdown, Fig. 3C). Non-degradable dex-MA nanogels were not able to silence the firefly luciferase gene to an appreciable extent (**supplementary information\_Fig. S2**). Note that the higher the DS of the nanogels the longer it takes to become degraded, while dex-MA based nanogels do not degrade at all [27]. It can be hypothesized that the DS 8.9 nanogels, when compared to DS 2.5 and DS 5.2, degrade too slow which could have its implications on the intracellular release of siRNA. Also, Table 1 and Fig. 2 showed a significantly lower zeta-potential and siRNA complexation capacity for the DS 8.9 nanogels; the lower positive surface charge of the DS 8.9 nanogels may result in a less efficient cellular internalization. Less uptake of DS 8.9 nanogels by Huh-7 cells could indeed be confirmed by flow cytometry (data not shown) and is therefore one of the reasons which explains the lower gene silencing by DS 8.9 nanogels.

None of the siRNA loaded nanogels was able to maintain sufficient gene silencing up to 7 days. The DS 2.5 nanogels (Fig. 3A), DS 5.2 nanogels (Fig. 3B) and Lipofectamine™RNAiMAX (Fig. 3D) achieved a maximal gene silencing of > 75% two days post-transfection. This level of gene suppression was maintained for an additional 24 h at most. Five days post-transfection, on average gene expression has recovered to ~50% compared to control, and seven days post-transfection, in most cases little gene suppression remains. From these data we conclude that the initial crosslink density of the nanogels apparently has an important effect on the extent of gene silencing though has little to no influence on the duration of the silencing.

We next evaluated the silencing of enhanced green fluorescent protein (EGFP) stably expressed in Huh-7\_EGFP cells [27]. **Fig. 4A-C** proves that dextran nanogels loaded with siRNA targeting the EGFP gene, were able to reduce the EGFP expression significantly. Fig. 4 also confirms the sequence-specificity of the downregulation effect, since none of the controls, i.e. empty nanogels and nanogels loaded with either a universal control siRNA (siCONTROL) or an irrelevant but validated siRNA (siLUC), reduced EGFP expression. A dose response experiment with DS 5.2 nanogels demonstrated a clear influence of the amount of siRNA used on the knockdown efficiency with an eventual IC<sub>50</sub> value ~1 pmol/mL siRNA under the experimental conditions (Fig. 4B). A time-dependent gene silencing experiment (Fig. 4D) lead to the observation that the extent of EGFP silencing significantly differs between the nanogels while the recovery of the EGFP expression is rather similar for all nanogels, in agreement with what we observed in the luciferase knockdown experiments in Fig. 3. Taken together from the data in Fig. 3 and Fig. 4 we assume that the gene silencing kinetics is independent on the dex-HEMA nanogel characteristics and is most likely governed by cell division [14].

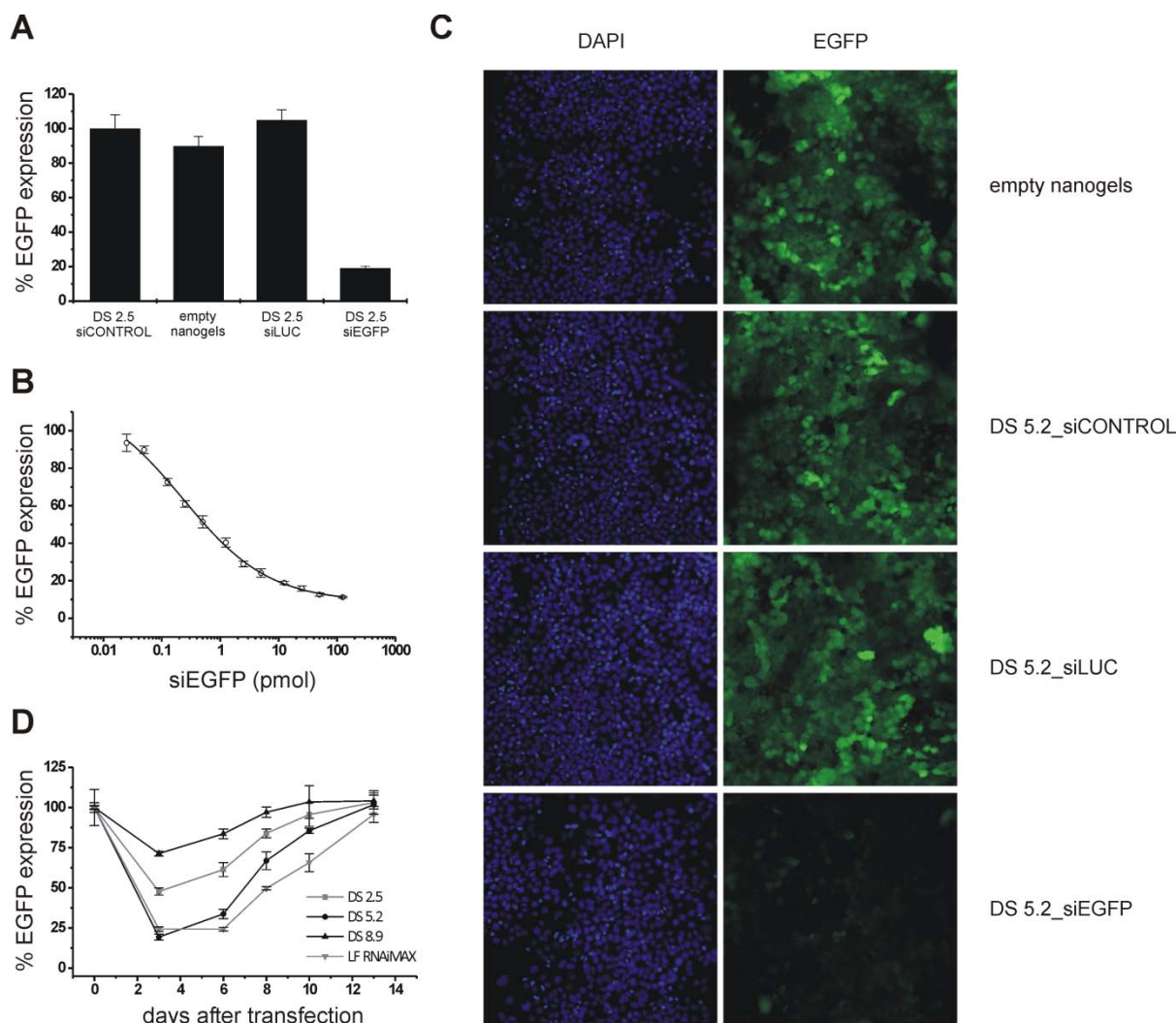


**Fig. 4. (A)** EGFP silencing by dex-HEMA DS 2.5 nanogels (60  $\mu\text{g}/\text{mL}$ ). Respectively empty nanogels (i.e. without siRNA) and nanogels loaded with control siRNA (siCONTROL, siLUC) or active siRNA (siEGFP) were used. The amount of siRNA added per well was 75 pmol per  $7.5 \times 10^4$  seeded cells in 12-well format and the EGFP expression was quantified 5 days post-transfection. **(B)** EGFP expression following transfection with dex-HEMA DS 5.2 nanogels (50  $\mu\text{g}/\text{mL}$ ) loaded with increasing amounts of siRNA. Data are shown as the amount of EGFP fluorescence in cells exposed to siEGFP nanogels relative to EGFP expression in cells exposed to siLUC nanogels (in %). Expression of EGFP was quantified 72 h post-transfection and transfection was performed in 24-well plates with  $3 \times 10^4$  seeded cells per well. **(C)** Visual control of EGFP silencing by DS 5.2 nanogels. In the left panel the cell nuclei are shown after staining with DAPI and the right panel shows the EGFP expression. **(D)** Time-dependent EGFP suppression in cells exposed to siEGFP loaded dex-HEMA-co-TMAEMA nanogels and siEGFP/lipofectamine<sup>TM</sup>RNAiMAX complexes. The concentration of nanogels was fixed to 50  $\mu\text{g}/\text{mL}$  and the amount of siRNA per well equalled 50 pmol (24-well plate).

Although siRNA loaded dex-HEMA nanogels significantly suppress gene expression in hepatoma cells we did observe that the majority of internalized siRNA-nanogels accumulates in acidified vesicles, which significantly hampers the cytoplasmic delivery of siRNA [22]. We

hypothesize that following cellular uptake only a small fraction of the siRNA molecules complexed to the nanogels reaches the cell cytoplasm and becomes available for incorporation into the RNAi pathway [22]. Indeed, also other reports in literature suggest that only a minor fraction of the siRNA transported across the cellular membrane by non-viral carriers is eventually responsible for the RNAi effect [29-32].

To improve the release of siRNA into the cytosol it is thus imperative to stimulate the escape of siRNA loaded nanogels from the endosomal compartment into the cytoplasm of the cell. Our previous data showed that photochemical internalization (PCI) can enhance the extent of gene silencing obtained with dex-HEMA nanogels [22]. PCI involves the use of amphiphilic photosensitizers (PS) that preferentially localize in the membrane of endocytic vesicles following cellular internalization (**supplementary information Fig. S3**). Excitation of the PS disrupts the membranes of intracellular vesicles, thereby triggering the release of internalized matter [23-25]. As described in the supplementary information (**Fig. S4**) we could visually confirm that PCI improves the intracytoplasmic siRNA delivery from dextran nanogels. In agreement with our earlier results we also observed a significant improvement in the extent of EGFP gene silencing when siEGFP loaded nanogels were used (data not shown).

More importantly, we now wanted to test whether PCI, besides improving the magnitude of gene silencing, would also allow to induce a more sustained gene silencing by siRNA delivered from dextran nanogels. In most therapeutic applications up to now, PCI is applied at the same day as the actual transfection. To the best of our knowledge, there are no PCI reports available addressing the activation of PS at later time-points post-transfection. Therefore we applied PCI at different time-points after transfecting the Huh-7\_EGFP cells with siRNA-nanogels (PCI applied at  $y$  days post-transfection is indicated as PCI <sub>$y$</sub> ) and analyzed the extent and duration of the gene silencing. The experimental protocols used in these experiments are summarized in supplementary information (**Fig. S5**).

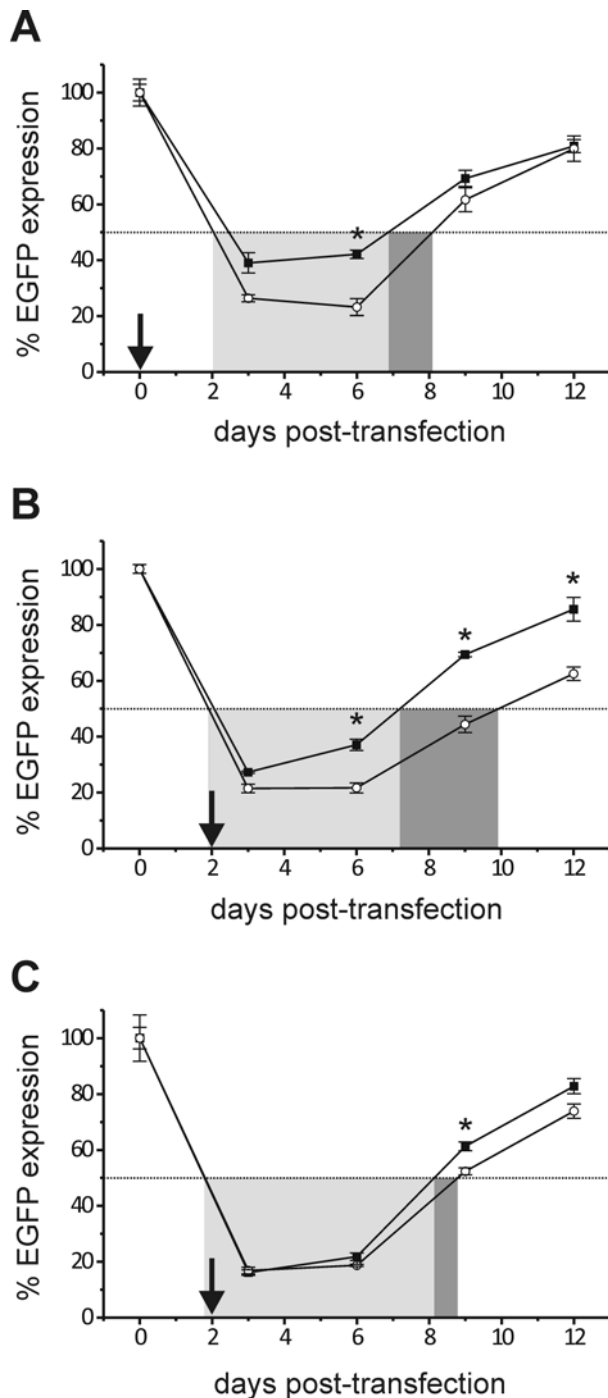


**Fig. 5.** EGFP expression as a function of time following transfection with siEGFP nanogels (DS 5.2) in the absence (■) or presence (○) of PS following the experimental protocol described in Fig. S5 in supplementary information. The arrow indicates the time-point of PS activation and PS was added to the cells one day prior to illumination. The (light and dark) grey colored zones indicate the time window during which more than 50 % knockdown of EGFP was observed. **(A)** 25  $\mu\text{g}/\text{mL}$  nanogels, PCI t0, **(B)** 25  $\mu\text{g}/\text{mL}$  nanogels, PCI t2, **(C)** 50  $\mu\text{g}/\text{mL}$  nanogels, PCI t2. Data points are mean values  $\pm$  SD (n=3). Data points where EGFP expression is statistically different (PCI compared with absence of PCI) are denoted by \* ( $p < 0.01$ ).



As **Fig. 5A** shows, PCI t0 on dex-HEMA-co-TMAEMA nanogels (DS 5.2, 25  $\mu\text{g}/\text{mL}$ ) markedly enhanced the EGFP knockdown. Nevertheless, the stronger gene silencing was gradually lost as can be seen at day 9 and day 12 post-transfection. Surprisingly, though importantly, when transfecting the cells with a higher nanogel concentration (50  $\mu\text{g}/\text{mL}$ ) the PCI t0 protocol did not enhance the gene silencing outcome (data not shown), indicating the saturation of the RNAi pathway when 50  $\mu\text{g}/\text{mL}$  was used. It seems that siRNA molecules additionally released into the cytoplasm by PCI treatment do not contribute to the RNAi effect but are merely diluted in the cell over time as a result of degradation and cell division. Hence, there is also no positive outcome on the longevity of the RNAi effect. To significantly prolong the RNAi effect, an additional siRNA dose will be needed at a later time following transfection. Therefore we further investigated whether delayed PCI could fulfil these requirements.

The results on the delayed PCI treatment (PCI t2) are summarized in Fig. 5B-C. At day 3 post-transfection, being 24 h after photochemical treatment, a (significant) difference is observed between PCI treated and non-treated cells when 25  $\mu\text{g}/\text{mL}$  nanogels were applied on the cells (Fig. 5B), but not when 50  $\mu\text{g}/\text{mL}$  nanogels were applied (Fig. 5C). At later time points the gene silencing remains substantially enhanced for the 25  $\mu\text{g}/\text{mL}$  transfected cells. These results clearly indicate that 2 days following transfection, PCI is still able to release some of the siRNA loaded nanogels into the cytosol. Most likely, newly formed PS containing vesicles can interact/fuse with pre-existing vesicles still containing siRNA nanogels thus explaining the additional RNAi effect following PS activation at t2.

This result also suggests that the prolonged residence time of siRNA duplexes in intracellular vesicles (e.g. endolysosomes) is not detrimental at least for a fraction of the internalized siRNAs. Nonetheless, as seen for PCI t0, PCI t2 can only moderately lengthen the EGFP knockdown (Fig. 5B).

Ideally an additional siRNA dose should be delivered in the cytosol at the time-point when maintaining the gene silencing effect becomes critical, i.e.  $\sim 6$  days under our experimental conditions as shown in Fig. 5. In fast dividing cell lines it is conceivable that the intracellular dilution of internalized nanogels, due to cell division, will set the limit for a delayed PCI treatment as sufficient nanogels should remain in the cells at the time of PCI. We studied the dilution of nanogels in Huh-7\_EGFP cells using Alexa Fluor<sup>®</sup>647 (AF647)-labelled cationic dex-MA nanogels (DS 5.9, 50  $\mu\text{g}/\text{mL}$ ). As **Fig. 6A** shows, the fluorescently labelled nanogels became easily internalized by hepatoma cells. The effect of cellular dilution could be clearly illustrated by flow cytometry measurements. Figure 6B reveals a fast decrease over time of the average intracellular fluorescence due to the distribution of the nanogel particles over the daughter cells. At day 6 post-transfection, only  $\sim 8\%$  of the initial average fluorescence remained although still 97% of the cells were positive for AF647 fluorescence.

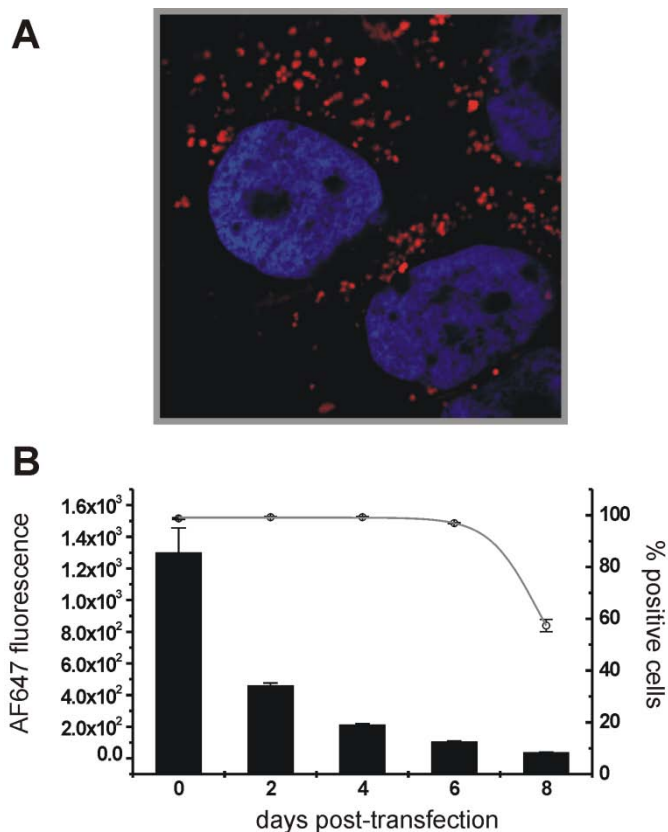


**Fig. 6. (A)** Confocal fluorescence image of Alexa Fluor<sup>®</sup>647 (AF647) labelled dex-MA-co-TMAEMA/AEMA nanogels (50 µg/mL, see Supplementary Information) internalized by Huh-7\_EGFP cells following 4 h of incubation. Nuclei are stained with DAPI (blue color). **(B)** Average Alexa Fluor<sup>®</sup>647 fluorescence of the cells (bars) and percentage of Alexa Fluor<sup>®</sup>647 positive cells (○) as a function of time after applying the red labeled nanogels, as measured by flow cytometry (n=6).

We therefore conducted a delayed PCI experiment on day 6 after transfection of Huh-7\_EGFP cells with siRNA loaded dex-HEMA-co-TMAEMA nanogels (DS 5.2, 50 µg/mL; see **Fig. S6** in supplementary information for experimental protocol). Lipofectamine<sup>™</sup>RNAiMAX was used as a control (**Fig. 7**). Also note that the PCI\_t6 experiment was performed with Dicer substrate siRNAs (DsiRNAs), chemically modified with 2'-O-methylribonucleotides [33], to provide additional stability against nuclease attack.

Without PCI (Fig. 7A), using both dex-HEMA-co-TMAEMA nanogels and Lipofectamine<sup>™</sup>RNAiMAX, the EGFP gene was silenced up to ~80% and this effect lasted for approximately 6 days after which the EGFP expression gradually recovered to steady state. Remarkably, the application of PCI 6 days post-transfection (Fig. 7B) substantially prolonged the gene silencing in cells transfected with the dextran nanogels, maintaining >50% EGFP downregulation for up to 2 weeks in the fast dividing cancer cells. This is much longer than the RNAi effect that is usually obtained in these cell lines [14]. It can be anticipated that when applying the same delivery strategy on cells with a slower division rate, even stronger effects could emerge.

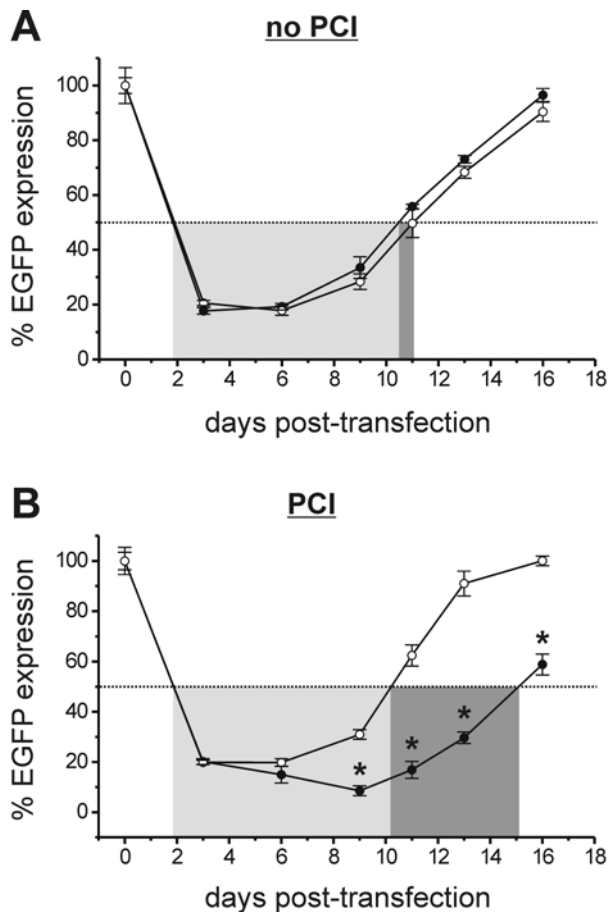


**Fig. 7. (A)** Application of PCI 6 days post-transfection (PCI t6) on cells transfected with dex-HEMA-co-TMAEMA (DS 5.2; 50  $\mu\text{g}/\text{mL}$ ) nanogels (●) and Lipofectamine™ RNAiMAX (○). (A) EGFP gene silencing as a function of time without PCI. (B) EGFP suppression as a function of time with the application of PCI. The (light and dark) grey colored zones indicate the time window during which more than 50 % knockdown of EGFP was observed. Data points where EGFP expression is statistically different compared with the same time-points in the transfection without PCI are denoted by \* ( $p < 0.005$ ).

In contrast and even more remarkable, this beneficial effect was not observed for the Lipofectamine™ RNAiMAX transfected cells. Also note that PCI t2 did not have a beneficial effect at all on the RNAi kinetics for Lipofectamine™ RNAiMAX (**supplementary information\_Fig. S7**). These data clearly reflect the difference in mechanism of siRNA delivery between a polymeric matrix type carrier (e.g. nanogels) and a lipid vesicle type carrier. Liposomal carriers most likely give rise to an immediate release of the loaded siRNA in the cytosol due to fusion with the endosomal membrane and even with the plasmamembrane [30]. Opposite to our nanogels, which remain trapped inside intracellular vesicles, liposomes do not create an intracellular depot of siRNA, thus making these transfection agents refractive towards a PCI controlled siRNA release.

It is important to note that in Fig. 7 chemically modified dicer substrate siRNAs (DsiRNAs) were used. DsiRNAs potentially show improved silencing efficiency and duration compared to conventional 21 mer siRNAs. This is thought to originate from Dicer recognition and

cleavage which could improve their incorporation into RISC. Moreover, the introduction of chemical modifications to decrease their susceptibility for nuclease degradation could also have its implications on the persistence of the RNAi effect relative to unmodified duplexes [13]. Especially following a prolonged incubation in the (nuclease rich) intracellular environment, the use of chemically modified DsiRNAs could be an advantage over unmodified 21 mer siRNAs.

On the other hand, also the electrostatic incorporation of siRNAs in dextran nanogel particles could provide additional protection to nuclease attack. At this moment we do not have conclusive data on the degradation of the DS 5.2 nanogels in the endolysosomal compartment. Early data in the literature [28] state that hydrolysis of the dex-HEMA carbonate ester is minimal at the acidic pH found in endolysosomes (pH ~4.5-5) and as a consequence the nanogel degradation will be substantially slower than at neutral pH. It still remains to be evaluated if after 6 days siRNA nanogels or decomplexed (free) siRNA is released into the cytoplasm.

## Conclusion

Photochemical internalization is able to liberate a fraction of the siRNA-nanogels trapped in (endocytic) vesicles, resulting in an additional siRNA dose that is released in the cell cytoplasm. PCI has the ability to substantially enhance the duration of EGFP knockdown, especially when PCI is applied at the time-point when maintaining the RNAi effect becomes critical. Delayed PCI therefore is a potential strategy to prolong the therapeutic effect in the case when endosomal escape is the effect-limiting step, by applying intracellular vesicles as depot systems for PCI controlled release. Moreover, this strategy enables longer RNAi effects to be obtained with one single dose of siRNA nanocarrier, thereby avoiding the need for a second administration to obtain the same effect longevity. The incorporation of the photosensitizing agent into the nanocarrier itself could be a valuable addition to this concept [34]. The siRNA impregnated nanogels are scheduled to be tested *in vivo* following local injection in combination with PCI at different time-points following administration.

## Acknowledgment

The authors acknowledge the EU (FP6) for funding of MediTrans, an integrated project on nanomedicines. Brian Sproat is thanked for providing the chemically modified DsiRNAs. A. Høgset is supported by the Norwegian Research Council.

## References

- [1] A. Fire, S. Xu, M.K. Montgomery, S.A. Kostas, S.E. Driver, C.C. Mello, Potent and specific genetic interference by double-stranded RNA in *Caenorhabditis elegans*, *Nature* 391 (1998) 806-811.
- [2] K.A. Whitehead, R. Langer, D.G. Anderson, Knocking down barriers: advances in siRNA delivery, *Nature Reviews Drug Discovery* 8 (2009) 129-138.

- [3] A.R. de Fougerolles, Delivery vehicles for small interfering RNA in vivo, *Hum. Gene Ther.* 19 (2008) 125-132.
- [4] M.E. Davis, The First Targeted Delivery of siRNA in Humans via a Self-Assembling, Cyclodextrin Polymer-Based Nanoparticle: From Concept to Clinic, *Mol. Pharm.* 6 (2009) 659-668.
- [5] M.A. Behlke, Chemical modification of siRNAs for in vivo use, *Oligonucleotides.* 18 (2008) 305-319.
- [6] E. Hefner, K. Clark, C. Whitman, M.A. Behlke, S.D. Rose, A.S. Peek, T. Rubio, Increased potency and longevity of gene silencing using validated Dicer substrates, *J. Biomol. Tech.* 19 (2008) 231-237.
- [7] M. Amarzguioui, J.J. Rossi, Principles of Dicer substrate (D-siRNA) design and function, *Methods Mol. Biol.* 442 (2008) 3-10.
- [8] C.Y. Chu, T.M. Rana, Potent RNAi by short RNA triggers, *RNA.* 14 (2008) 1714-1719.
- [9] M. Sano, M. Sierant, M. Miyagishi, M. Nakanishi, Y. Takagi, S. Sutou, Effect of asymmetric terminal structures of short RNA duplexes on the RNA interference activity and strand selection, *Nucleic Acids Res.* 36 (2008) 5812-5821.
- [10] K. Gao, L. Huang, Nonviral Methods for siRNA Delivery, *Mol. Pharm.* 6 (2009) 651-658.
- [11] T.I. Novobrantseva, A. Akinc, A. Borodovsky, F.A. de, Delivering silence: advancements in developing siRNA therapeutics, *Curr. Opin. Drug Discov. Devel.* 11 (2008) 217-224.
- [12] D. Peer, E.J. Park, Y. Morishita, C.V. Carman, M. Shimaoka, Systemic leukocyte-directed siRNA delivery revealing cyclin D1 as an anti-inflammatory target, *Science* 319 (2008) 627-630.
- [13] K. Raemdonck, R.E. Vandenbroucke, J. Demeester, N.N. Sanders, S.C. De Smedt, Maintaining the silence: reflections on long-term RNAi, *Drug Discovery Today* 13 (2008) 917-931.
- [14] D.W. Bartlett, M.E. Davis, Insights into the kinetics of siRNA-mediated gene silencing from live-cell and live-animal bioluminescent imaging, *Nucleic Acids Research* 34 (2006) 322-333.
- [15] A. Mantei, S. Rutz, M. Janke, D. Kirchhoff, U. Jung, V. Patzel, U. Vogel, T. Rudel, I. Andreou, M. Weber, A. Scheffold, siRNA stabilization prolongs gene knockdown in primary T lymphocytes, *Eur. J. Immunol.* 38 (2008) 2616-2625.
- [16] A.A. Volkov, N.S. Kruglova, M.I. Meschaninova, A.G. Venyaminova, M.A. Zenkova, V.V. Vlassov, E.L. Chernolovskaya, Selective Protection of Nuclease-Sensitive Sites in siRNA Prolongs Silencing Effect, *Oligonucleotides* 19 (2009) 191-202.
- [17] A. Judge, I. Maclachlan, Overcoming the innate immune response to small interfering RNA, *Human Gene Therapy* 19 (2008) 111-124.

- [18] P. Svoboda, Off-targeting and other non-specific effects of RNAi experiments in mammalian cells, *Current Opinion in Molecular Therapeutics* 9 (2007) 248-257.
- [19] D. Grimm, K.L. Streetz, C.L. Jopling, T.A. Storm, K. Pandey, C.R. Davis, P. Marion, F. Salazar, M.A. Kay, Fatality in mice due to oversaturation of cellular microRNA/short hairpin RNA pathways, *Nature* 441 (2006) 537-541.
- [20] D.M. Dykxhoorn, J. Lieberman, Knocking down disease with siRNAs, *Cell* 126 (2006) 231-235.
- [21] K. Raemdonck, J. Demeester, S. De Smedt, Advanced nanogel engineering for drug delivery, *Soft Matter* 5 (2009) 707-715.
- [22] K. Raemdonck, B. Naeye, K. Buyens, R.E. Vandenbroucke, A. Hogset, J. Demeester, S.C. De Smedt, Biodegradable Dextran Nanogels for RNA Interference: Focusing on Endosomal Escape and Intracellular siRNA Delivery, *Advanced Functional Materials* 19 (2009) 1406-1415.
- [23] K. Berg, M. Folini, L. Prasmickaite, P.K. Selbo, A. Bonsted, B.O. Engesaeter, N. Zaffaroni, A. Weyergang, A. Dietze, G.M. Maelandsmo, E. Wagner, O.J. Norum, A. Hogset, Photochemical internalization: a new tool for drug delivery, *Curr. Pharm. Biotechnol.* 8 (2007) 362-372.
- [24] K.G. de Bruin, C. Fella, M. Ogris, E. Wagner, N. Ruthardt, C. Brauchle, Dynamics of photoinduced endosomal release of polyplexes, *J. Control Release* 130 (2008) 175-182.
- [25] S. Oliveira, A. Hogset, G. Storm, R.M. Schifflers, Delivery of siRNA to the target cell cytoplasm: photochemical internalization facilitates endosomal escape and improves silencing efficiency, *in vitro and in vivo*, *Curr. Pharm. Des* 14 (2008) 3686-3697.
- [26] L. Prasmickaite, A. Hogset, P.K. Selbo, B.O. Engesaeter, M. Hellum, K. Berg, Photochemical disruption of endocytic vesicles before delivery of drugs: a new strategy for cancer therapy, *Br. J. Cancer* 86 (2002) 652-657.
- [27] K. Raemdonck, T.G. Van Thienen, R.E. Vandenbroucke, N.N. Sanders, J. Demeester, S.C. De Smedt, Dextran microgels for time-controlled delivery of siRNA, *Advanced Functional Materials* 18 (2008) 993-1001.
- [28] W.N. Van Dijk-Wolthuis, M.J. van Steenberg, W.J. Underberg, W.E. Hennink, Degradation kinetics of methacrylated dextrans in aqueous solution, *J. Pharm. Sci.* 86 (1997) 413-417.
- [29] A. Detzer, M. Overhoff, W. Wunsche, M. Rompf, J.J. Turner, G.D. Ivanova, M.J. Gait, G. Sczakiel, Increased RNAi is related to intracellular release of siRNA via a covalently attached signal peptide, *RNA*. 15 (2009) 627-636.
- [30] J.J. Lu, R. Langer, J. Chen, A Novel Mechanism Is Involved in Cationic Lipid-Mediated Functional siRNA Delivery, *Mol. Pharm.* 6 (2009) 763-771.

- [31] A. Mescalchin, A. Detzer, M. Wecke, M. Overhoff, W. Wunsche, G. Sczakiel, Cellular uptake and intracellular release are major obstacles to the therapeutic application of siRNA: novel options by phosphorothioate-stimulated delivery, *Expert. Opin. Biol. Ther.* 7 (2007) 1531-1538.
- [32] S. Veldhoen, S.D. Laufer, A. Trampe, T. Restle, Cellular delivery of small interfering RNA by a non-covalently attached cell-penetrating peptide: quantitative analysis of uptake and biological effect, *Nucleic Acids Res.* 34 (2006) 6561-6573.
- [33] M.A. Collingwood, S.D. Rose, L. Huang, C. Hillier, M. Amarzguioui, M.T. Wiiger, H.S. Soifer, J.J. Rossi, M.A. Behlke, Chemical modification patterns compatible with high potency dicer-substrate small interfering RNAs, *Oligonucleotides.* 18 (2008) 187-200.
- [34] N. Nishiyama, A. Iriyama, W.D. Jang, K. Miyata, K. Itaka, Y. Inoue, H. Takahashi, Y. Yanagi, Y. Tamaki, H. Koyama, K. Kataoka, Light-induced gene transfer from packaged DNA enveloped in a dendrimeric photosensitizer, *Nature Materials* 4 (2005) 934-941.